Ren *et al.*
Food Production, Processing and Nutrition (2024) 6:6
https://doi.org/10.1186/s43014-023-00180-x

Food Production, Processing and Nutrition

RESEARCH

Open Access

Identification and molecular mapping of resistance genes for adult-plant resistance to stripe rust in spring wheat germplasm line PI660076

Runsheng Ren[1,2†], Jianian Zhou[3†], Yuqi Wang[3], Lirong Wang[3], Xiaochen Zheng[3], Xin Li[3], Suizhuang Yang[3], Xinli Zhou[3*] and Pingping Zhang[1,4,5*]

Abstract

Wheat is one of the major food crops worldwide. Stripe rust can cause a great loss of wheat yield, especially when the disease is prevalent. Chemical control not only causes the loss of resistance to stripe rust but also has a serious impact on the human body and environment. Therefore, the most economical measure to control wheat stripe rust is to cultivate resistant varieties. Rapid variation of stripe rust races often leads to rapid "loss" of resistance to stripe rust disease; therefore, breeders and researchers have to continuously explore new stripe rust resistance genes to provide new resistance sources for the rapid variation of stripe rust races. Previous studies have confirmed that PI660076, a spring wheat line, showed stripe rust resistance under natural conditions at the adult stage, which has great value in breeding programs. In this study, a recombinant inbred lines (RIL) population was constructed by crossing the wheat line PI660076 with the stripe rust-susceptible line AvS. Genotyping of the population was performed using a wheat 15 K SNP array. Three QTLs were identified using phenotypic data over four years across three environments. The resistance type of each QTL was determined by inoculating the RIL lines with single and homozygous QTL during the seedling and adult stages under controlled conditions. The all-stage resistance (ASR) QTL, *QYr076.jaas-2A* (flanked by SNP marker *AX-11048464* and Kompetitive Allele-Specific PCR (KASP) marker *KASP_4940*) explained 7.13–16.58% and 6.95–7.25% of infection type (IT) and disease severity (DS), respectively. The adult-plant resistance (APR) resistance QTL, *QYr076.jaas-4D.1* (flanked by KASP marker *KASP_0795* and SNP marker *AX-111567243*,) explained 6.85–12.70% and 7.94–17.26% of IT and DS, respectively. The APR resistance QTL, *QYr076.jaas-4D.2* flanked by KASP markers *KASP_9130* and *KASP_6535*, explained 7.97–39.19% and 8.77–20.55% of the phenotypic variation in IT and DS, respectively. All the three QTLs are likely to be new. The obtained results lay a foundation for further utilization of the stripe rust-resistant line PI660076, as well as for fine mapping and molecular marker-assisted selection breeding.

Keywords Wheat, Stripe rust, Adult-plant resistance, Molecular mapping, QTL

†Runsheng Ren and Jianian Zhou contributed equally to this work.

*Correspondence:
Xinli Zhou
eli6951@sina.com
Pingping Zhang
pzh@jaas.ac.cn
Full list of author information is available at the end of the article

Graphical Abstract

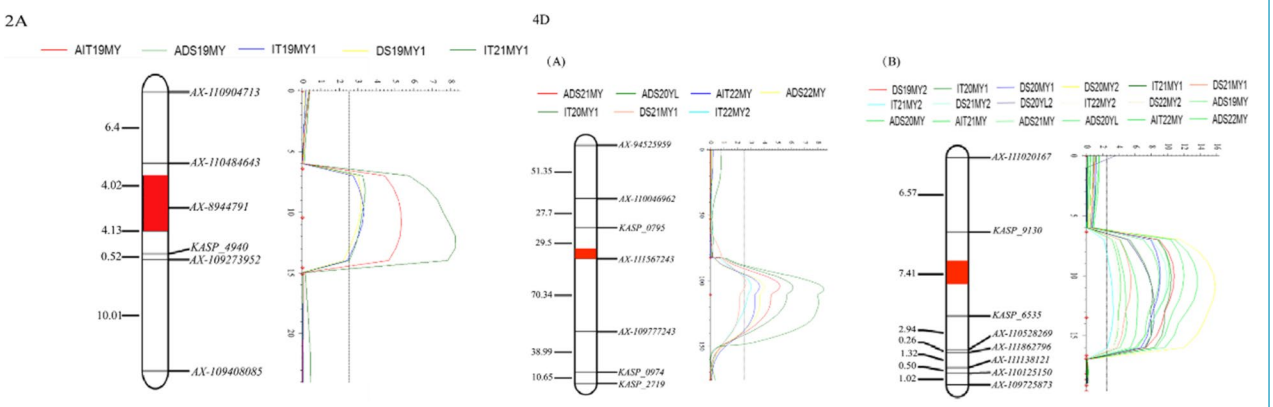

Introduction

Stripe rust, caused by *Puccinia striiformis* f. sp. *tritici* (*Pst*), is a typical airborne disease that can spread with high air flow and occurs in almost all wheat growing areas in the world. Once wheat stripe rust breaks out, it will seriously interfere with the normal growth of wheat. In the epidemic year, it will cause serious yield loss and economic loss to wheat production (Chen 2014; Zhou et al. 2022a). Currently, there are two main control strategies for wheat stripe rust. One is chemical control, which has the advantages of quick effect and strong results. Especially in the year of the stripe rust epidemic, it can effectively reduce the loss of wheat yield. However, this method also has clear weakness; specifically, long-term use will not only make the pathogen produce fungicide resistance but will also have an impact on the environment and human health. Compared with chemical control, planting disease-resistant varieties is the most economic and environmentally friendly method; however, the loss of resistance to stripe rust is caused by virulence variation of stripe rust, which is a major problem in resistant breeding programs (Line 2002).

Many stripe rust resistance genes lost effectiveness within a few years due to racial variation in pathogen populations, such as *Yr1-Yr4*, *Yr6-Yr10*, *Yr17*, *Yr20-Yr22*, *Yr24-Yr29* and *Yr43* (Chen 2020). These resistance genes belong to the all-stage resistance (ASR) type (also referred to as seedling resistance), which has the disadvantage of being race specific. In contrast, the other type of resistance, adult-plant resistance (APR), has the characteristics of being nonrace-specific and therefore more durable, which can effectively delay the speed of 'loss' of resistance in wheat varieties, such as the wheat cultivar Libellula grown in Longnan, Gansu, China (Zhou et al. 2003) and Alpowa grown in the US Pacific Northwest (Lin & Chen 2007). To date, 84 officially named stripe rust resistance genes and more than 200 QTLs have been identified, most of which belong to ASR, and only a few are APR (Feng et al. 2018; Klymiuk et al. 2022; Ren et al. 2012a; Wang et al. 2022; Zhou et al. 2014, 2022b). Therefore, it is important to identify more APR resistance genes in wheat and its close wild relatives.

PI660076 is a spring wheat line obtained by crossing stripe rust resistance donor PI180957 and stripe rust susceptible wheat cultivar 'Avocet Susceptible (AvS)' in USDA-ARS, Wheat Genetics, Quality, Physiology and Disease Research Unit (Wang et al. 2012). Previous studies have found that PI660076 was susceptible at the seedling stage and resistant at the adult stage, with the exception of Tianshui, Gansu Province, China, in 2013, which showed that PI660076 was susceptible in the field at the adult stage (unpublished data). For this interesting situation, one conjecture was that there was probably a race in the field of Tianshui in 2013, which could interact with a host gene in PI660076 and cause susceptibility, but during the next year, this race did not become dominant, and there was no corresponding race to interact with the host gene, resulting in resistance. However, because the races that caused susceptibility to PI660076 in the Tianshui field in 2013 were not collected and identified, there was no way to verify this susceptible phenotype. On the other hand, PI660076 showed resistance in the adult stage but susceptibility at the seedling stage, and it is necessary to identify and map its resistance QTL.

In this study, 208 F_7 generation recombinant inbred lines (RILs) were constructed by crossing PI660076 with AvS and were genotyped with the 15 K SNP array on a

whole genome scale. Combined with the genotypic variation and phenotypic identification of stripe rust in the field, molecular mapping of the stripe rust resistance gene in PI660076 was performed.

Materials and methods

Plant materials and stripe rust evaluation in field

A RIL population with 208 lines was produced by crossing the stripe rust-susceptible wheat cultivar AvS as the female parent with PI660076 as the donor of stripe rust resistance. The RIL population and the two parents were tested for their reaction to naturally occurring stripe rust in the field at Mianyang (MY), Sichuan in 2019, 2020, 2021 and 2022, and Yangling (YL), Shannxi in 2020. In these field trials, each trial was designed by a random complete block design, with three repetitions at each location. Each trial plot was composed of a single row with a length of 1m, and the distance between adjacent rows was 25cm. Each plot was seeded with approximately 40 seeds of a RIL, and a group of parents was seeded every 60 rows to detect the uniformity of stripe rust infection. A row of AvS was sown around each block and served as induced plants for stripe rust. The infection type (IT) and disease severity (DS) data were collected when the susceptible parent AvS and some susceptible lines of the RIL population were fully infected. The classification standard of infection type (IT) is based on the 0–9 scale. The disease severity (DS) refers to the percentage of disease area in leaves (classified by 0%, 1%, 5%, 10%, 20%, 30%, 40%, 50%, 60%, 70%, 80%, 90%, 100%).

Greenhouse test

Two parents and the RIL lines with single and homozygous QTL were selected for seedling test and adult test. Two-leaf stage seedlings and adult plant (flag leaf fully developed) of the lines were inoculated with mixed *Pst* races collected from infected wheat plants in field. About 10 seeds of each line and parents were planted in a 7×7×7cm pot filled with soil mixture and grown in a rust-free growth chamber. The inoculated plants were kept in a dew chamber for 24h at 10 C without light, and then the seedling plants were grown in a growth chamber using a low diurnal temperature cycle gradually changing between 4 C at 2:00 am and 20 C at 2:00 pm with 16h light/8h dark. For the adult plants after inoculation, they were grown under controlled conditons using a low diurnal cycle of temperatures gradually changing from 4 C to 20 C and a high diurnal cycle from 10 C to 35 C. Infection type (IT) based on the 0–9 scale was scored for each line 18 to 21days after inoculation when stripe rust was fully developed on AvS.

DNA extraction

Approximately 2 g of young leaf tissue from each RIL and the parents was harvested and dried in a freeze dryer (Thermo Savant, Holbrook, NY, USA) for 48 h and ground using a Mixer Mill (MM 300, Retsch, Germany) for DNA isolation. After the completion of the DNA extraction using a CTAB method as modified by Zhou et al. (2021), DNA was dissolved in Tris–EDTA (10mM Tris–HCl and 1mM EDTA, pH 8.0) buffer. All DNA samples were quantified by an ND-1000 Spectrophotometer (NanoDrop Technologies, Thermo Scientific, Wilmington, DE, USA) and adjusted to a final concentration of 50ng/μl as stock DNA solutions. Stock DNA solutions were further diluted with sterilized ddH_2O depending on the requirements of the individual experiment.

Genetic map construction and QTL analysis

Genotyping analysis of the RIL population was performed using a wheat 15 K SNP chip assay, and a marker scoring matrix was created in Excel. For mapping analysis, the association between disease trait data and marker data was calculated by the inclusive composite interval mapping (ICIM) method with the software IciMapping v4.1 (Meng et al. 2015). Marker deletion was performed using the "Bin" function, and genetic mapping was performed with the Kosambi mapping function (Kosambi 2016). Phenotypic variation and correlation analysis were also calculated by SAS 9.0 (SAS Inc., Cary, NC). QTL analysis was performed on the basis of line means from individual experiments in each site-year environment. A threshold likelihood of odds (LOD) of 2.5 was set to claim the significance of the QTL ($P < 0.01$).

The physical location of the QTL was determined according to the physical locations of the SNP markers linked to the QTL. The IWGCS-RefSeq v1.1 was used as a reference to construct a physical map. MapChart v2.3 (Voorrips 2002) was used to draw the genetic and physical reference maps.

Exon capture sequencing analysis

DNA from the parental cultivars was used to perform exome capture sequencing using BGI T7 platform (150-bp paired-end reads) according to the wheat exome capture sequencing protocol described by Dong et al. (2020) by Tiancheng Weilai Technology Co., Ltd., (Chengdu, China). After removing adapter sequences, low-quality bases, or undetected bases, clean reads were aligned to the Chinese Spring (CS) reference genome (IWGSC RefSeq v2.1) with the BWA software (default parameters) (Li & Durbin 2009) and single nucleotide polymorphism (SNP) and short insertions and deletions (INDELs) were called using the GATK software (default parameters).

Development of KASP markers

Based on the physical positions of the SNPs obtained from the exon capture sequencing analysis, the SNPs in the targeted QTL intervals were converted to KASP markers. KASP primers were developed following standard KASP guidelines. The allele-specific primers were designed carrying the standard FAM (5′-GAAGGTGAC CAAGTTCATGCT-3′) and HEX (5′- GAAGGTCGG AGTCAACGGATT-3′) tails at the 3′ end of the targeted SNP. Common primers were designed so that the total amplicon length was less than 120 bp. KASP assays were performed in 96-well format in 10 µL reaction volumes containing 5 µL HiGeno 2×Probe Mix, 0.14 µL KASP primer mix (allele-specific primer 1-FAM (12 µM), allele-specific primer 2-HEX (12µM) and common reverse primer (30 µM)), 2 µL genomic DNA at 30 ng μL^{-1} and 3 µL ddH_2O. KASP reactions were carried out using Pherastar scanner (LGC Genomics, United Kingdom), with the following PCR cycling protocol: hot start at 95 °C for 10 min, followed by 10 touchdown cycles (95 C for 20 s; touchdown at 61 C initially and decreasing by 0.6 °C per cycle for 40s), followed by 30 additional cycles of annealing (95 C for 20 s; 55 C for 40 s).

Results

Phenotypic characterization of APR Resistance

In all three field trials, the plants in each trial were fully infected. The average IT and DS of the susceptible parent AvS were 8–9 and 91–100%, respectively, while those of the resistant parent PI660076 were 2–3 and 0–10%, respectively (Figs. 1 and 2). The distribution of the average IT and DS of the F_7 RIL population at the adult stage showed continuous unimodal distribution characteristics (Fig. 2), indicating that the disease resistance at the adult stage belonged to quantitative trait inheritance. Pearson correlation coefficients of the mean IT and DS of the F_7 RILs between different environments were all positive and highly significant ($P<0.001$) and ranged from 0.46 to 0.80 for IT and from 0.38 to 0.65 for DS (Table 1). The ANOVA showed that the variations in lines, environments and lines×environment for both the IT and DS (Table 2) were all significant ($P<0.001$) (Table 2), suggesting that the expression of APR resistance was consistent across the different environments and over different years. The broad sense heritability of IT and DS was 0.9 for IT and 0.83 for DS (Table 2), which indicated that the disease resistance at the adult stage was mainly determined by genotype and had stable gene expression.

Genetic linkage map construction

The wheat 15 K chip assay scanning results showed that a total of 3494 SNP markers were used for linkage map construction, giving a total map length of 14,025.4 cM, with individual chromosomes ranging from 473.5 cM for chromosome 6D to 828.9 cM for chromosome 3B (Table 3). The number of markers per chromosome ranged from 40 for chromosome 4B to 710 for chromosome 2A, with an average number of 166 SNP markers. The average distance between neighboring SNP markers ranged from 1.1 cM/marker for chromosome 2A to 16.8 cM/marker for chromosome 4B, with an average number of 6.9 cM/marker. The map was used to identify significant associations between SNP markers and stripe rust resistance.

Exon capture sequencing and development of KASP markers

In order to facilitate the use of QTL-linked markers, we first converted the flanking SNP markers of the QTLs into KASP markers. Although attempts were made to convert 6 SNP sites into KASP markers, only 3 SNP sites (all for the QTL on chromosomes 4D) could be successfully converted to KASP markers. The successfully converted SNP markers were *AX-89349130* (converted to *KASP_9130*), *AX-108766535* (converted to *KASP_6535*), and *AX-110080795* (converted to *KASP_0795)*. Therefore, in order to obtain more SNP markers, we did the exon capture sequencing of parental DNA. We selected the SNP sites within the mapping interval, and successfully developed three more KASP markers (*KASP_4940*, *KASP_2719*, *KASP_0974*). The newly developed KASP markers together with the other SNP markers were verified in the RIL population.

QTL for stripe rust resistance

Three major QTLs were consistently detected in the RIL population across 5 experiments on chromosomes 2A and 4D, and the one QTLs was temporarily named *QYr076.jaas-2A* (Fig. 3) and two QTLs on chromosome 4D were temporarily named *QYr076.jaas-4D.1* and *QYr076.jaas-4D.2* (Fig. 4). *QYr076.jaas*-2A was located between the SNP markers *AX-110484643* and KASP marker *KASP_4940* at LOD scores of 3.32–8.24, and its genetic distance was 4.13 cM (Table 4). This QTL explained 7.13-16.58% of the phenotypic variance explained (PVE). The physical locations of the two closely linked markers were 21.13 Mb and 27.90 Mb, respectively (Table 5). The flanking markers for QTL *QYr076.jaas-4D.1* were KASP marker *KASP_0795* and SNP marker *AX-111567243*, with *AX-111567243* as the closest marker to the QTL, and the PVEs were 6.85-12.70% (Table 4). Its physical location was 24.26 Mb and 46.99 Mb, respectively, and its genetic distance was 29.5 cM (Table 5). The

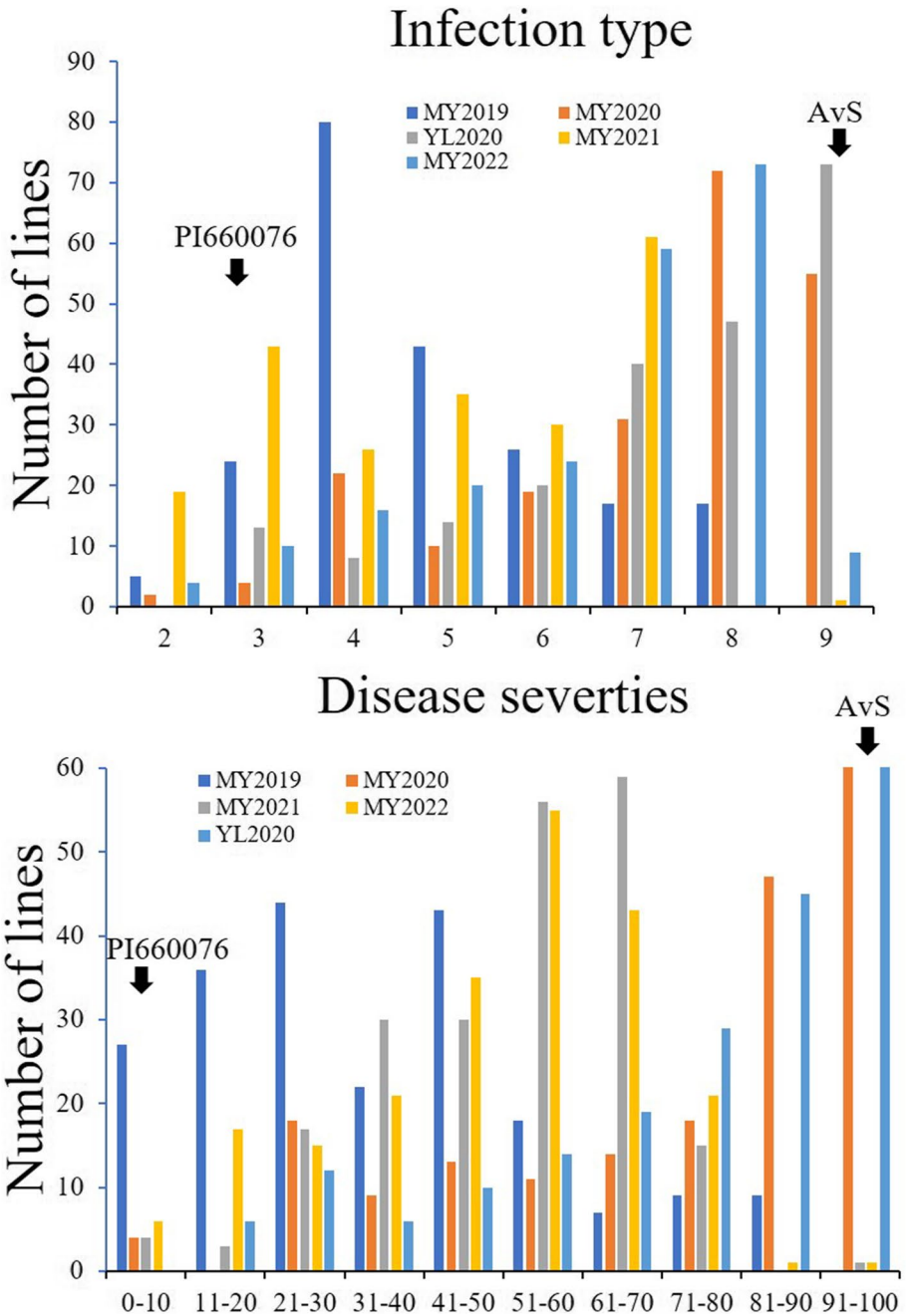

Fig. 1 Frequency distributions of the mean infection type (IT) and disease severity (DS) for 208 RILs from the AvS × PI660076 cross grown at Mianyang (MY) and Yangling (YL) in 2019–2022. Arrows indicate the values of the parental lines

flanking markers for QTL *QYr076.jaas-4D.2* were KASP markers *KASP_9130* and *KASP_6535*, with *KASP_9130* as the closest marker to the QTL, and the PVEs were 7.97-39.19% (Table 4). Its physical location was 379.78 Mb and 436.91 Mb, respectively, and its genetic distance was 7.41 cM (Table 5). The primer information of the KASP markers was provided in Table 6.

Determination of QTL resistance types

Based on the marker genotyping data for the RIL population, 49 homozygous lines containing only *QYr076.jaas-2A* locus, 43 homozygous lines containing only *QYr076.jaas-4D* loci (including *QYr076.jaas-4D.1* and *QYr076.jaas-4D.2*), and 47 homozygous lines containing both *QYr076.jaas-2A* locus and *QYr076.jaas-4D* loci were

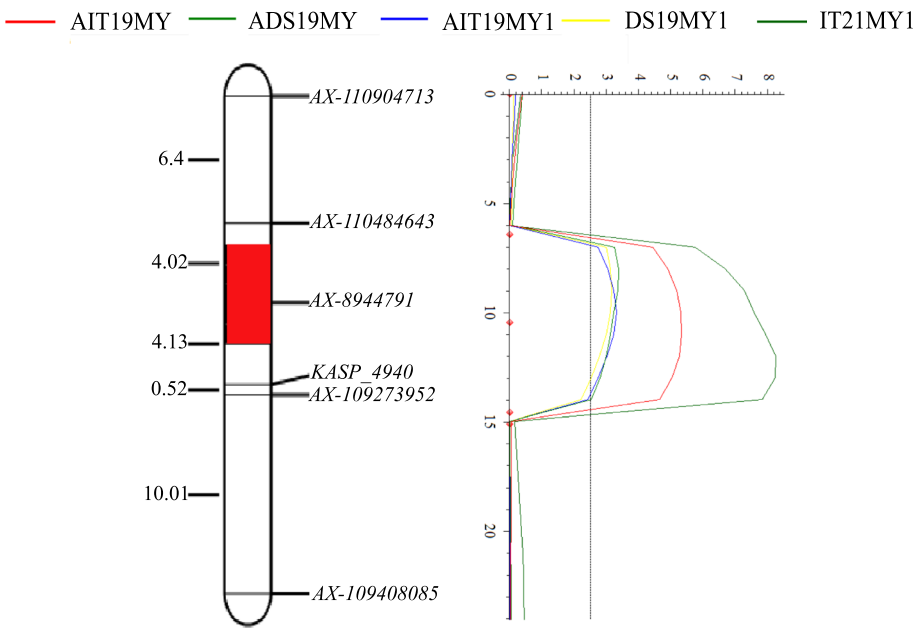

Fig. 2 Stripe rust resistance QTL on the genetic map of chromosomes 2A based on IT and DS data. The x-axis is in centimorgan distance (cM), and all genetic distance values shown are in the same scale; the y-axis indicates the LOD value. The red rectangle on the genetic map indicates the corresponding QTL region. AIT: average of IT. ADS: average of DS

selected for inoculation with mixed Chinese *Pst* (CYR31, CYR33, CYR34) at seedling stage and adult plant stage in controlled conditions. The results showed that all the 49 RIL lines containing *QYr076.jaas-2A* exhibited resistance at the seedling stage, such as line 6, line 9, line 68, line 125, and line 139 (Fig. 4A). All the 43 RIL lines containing QTLs on chromosome 4D showed resistance at the adult plant stage, such as line 72, line 98, line 103, line 115, line 116, and line 183 (Fig. 4B). All the 47 RIL lines containing both QTL loci exhibited resistance at both seedling stage and adult plant stage, such as line 22, line 56, line 124, line 126, and line 152 (Figs. 4A and B). Based on the inoculation results, we can preliminarily conclude that the resistance type of *QYr076.jaas-2A* belonged to ASR, and the QTLs on chromosome 4D are of APR. The relationships between the *QYr076.jaas-4D.1* and *QYr076.jaas-4D.2* need further exploration.

Discussion

In this study, we focused on the unidentified source of resistance in PI660076, a line originating from the USA. PI660076 maintains long-term disease resistance under natural conditions in an experimental field in Pullman, Washington, USA (unpublished). To test its resistance to Chinese predominant stripe rust races, PI660076

Table 1 Correlation coefficients (r) of the mean infection type (IT) and disease severity (DS) of the AvS × PI660076-derived recombinant inbred lines tested in different environments

	IT					DS (%)				
	19MY	20MY	21MY	22MY	20YL	19MY	20MY	21MY	22MY	20YL
19MY	1					1				
20MY	0.60 ***	1				0.52 ***	1			
21MY	0.48 ***	0.59 ***	1			0.48 ***	0.49 ***	1		
22MY	0.49 ***	0.49 ***	0.49 ***	1		0.51 ***	0.38 ***	0.56 ***	1	
20YL	0.60 ***	0.80 ***	0.58 ***	0.46 ***	1	0.64 ***	0.65 ***	0.64 ***	0.52 ***	1

The significance level was set at $P < 0.05$ (*), $P < 0.01$ (**), and $P < 0.001$ (***)

Table 2 Analysis of variance and estimation of broad-sense heritability of the infection type (IT) and disease severity (DS) among 208 RILs from the AvS × PI660076 cross tested in Mianyang (MY) and Yangling (YL) in 2019–2022

Source of variation	IT				DS (%)			
	Df	MS	F value	[c]Sig	Df	MS	F value	[c]Sig
Lines	207	17.9	13.6	***	207	2383.5	10.56	***
Block/Environments	5	166.6	127.9	***	5	35,776.1	158.5	***
Environments	4	1338.4	334.6	***	4	46,529.2	206.1	***
Lines × Environments	828	2382.0	2.8	***	828	441.2	1.9	***
Error	1485	1.3			1485	225.73		
[a]σ2g	1.37				179.89			
[b]H^2(broad-sense heritability)	0.9				0.83			

[a] σ2g was estimated for genotypic (line) variances

[b] H^2 indicates the estimated heritability in the broad sense on the basis of the mean across replications and environments (or heritability per mean)

[c] Significance level at $P < 0.05$ (*), $P < 0.01$ (**), $P < 0.001$ (***)

Table 3 Summary of chromosome assignment, number of SNP markers, map length, and marker density of the SNP genetic map of the 208 RILs from the AvS × PI660076 cross

Chromosome	Number of SNP markers	Map length in Mb	SNP intervals in cM
1A	219	592.3	2.03
1B	88	687.3	7.8
1D	73	494.7	6.8
2A	710	778.5	1.1
2B	75	799.8	10.7
2D	46	649.8	14.1
3A	292	750.3	2.6
3B	85	828.9	9.8
3D	101	614.1	6.1
4A	63	737.4	11.7
4B	40	672.9	16.8
4D	52	508.4	9.8
5A	338	709.4	2.1
5B	136	713.0	5.2
5D	187	562.5	3.0
6A	290	616.3	2.1
6B	84	715.9	8.5
6D	59	473.5	8.0
7A	319	735.4	2.3
7B	76	750.3	9.9
7D	161	634.7	3.9
Total	3494	14,025.4	-
Average	166	667.9	6.9

together with other wheat germplasm resources were introduced into China for stripe rust resistance testing. Through the identification of stripe rust resistance at the seedling stage and adult stage by Zhou et al. (2015), it was found that PI660076 showed no stripe rust symptoms on its leaves in many years from 2007 to the present in the infected field, whereas AvS consistently showed infection symptoms when grown at the same time and under the same conditions, except for the test in Tianshui in 2013, in which PI660076 showed a susceptible phenotype (IT = 8; DS = 80%). Interestingly, PI660076 still maintained good resistance in other years in Tianshui. Compared with other places at the same time and Tianshui in other years, one explanation is that there was a physiological race in the Tianshui area in 2013, and the stripe rust race could interact with genes in the host, which resulted in the original disease resistance genes becoming susceptible. This could be because that Tianshui is in the southwest China, which is suitable for suitable for overwintering and summering stripe rust. In other words, the Tianshui area belongs to the lair of Chinese stripe rust pathogens. Although this is an interesting phenomenon, there is currently no way to identify this susceptible gene. Because PI660076 maintained good stripe rust resistance over multiple years and locations in China, it is necessary to identify and map its resistance genes.

This study identified three QTLs for stripe rust resistance in the germplasm PI660076. The QTL *QYr076.jaas-2A* was located on the short arm of chromosome 2A. Chromosome 2A is rich in resistance QTLs and resistance genes, but almost all of the resistance genes that have been reported are ASR genes. Wheat chromosome 2AS is also a hot spot where genes for stripe rust resistance are enriched. Currently, this region contains more than 20 genes/QTLs having the characteristics of APR, including one officially named APR gene, *Yr17* (Bariana & McIntosh 1993), and 24 QTL with APR to stripe rust such as *QYr.inra-2A_CampRemy* (Mallard et al. 2005), *QYr.inra_2AS.1_Recital* (Dedryver et al. 2009), *QYr.sun-2A_Kukri* (Bariana et al. 2010), *QYrst.orr-2AS_Stephens* (Vazquez et al. 2015), *QYr.*

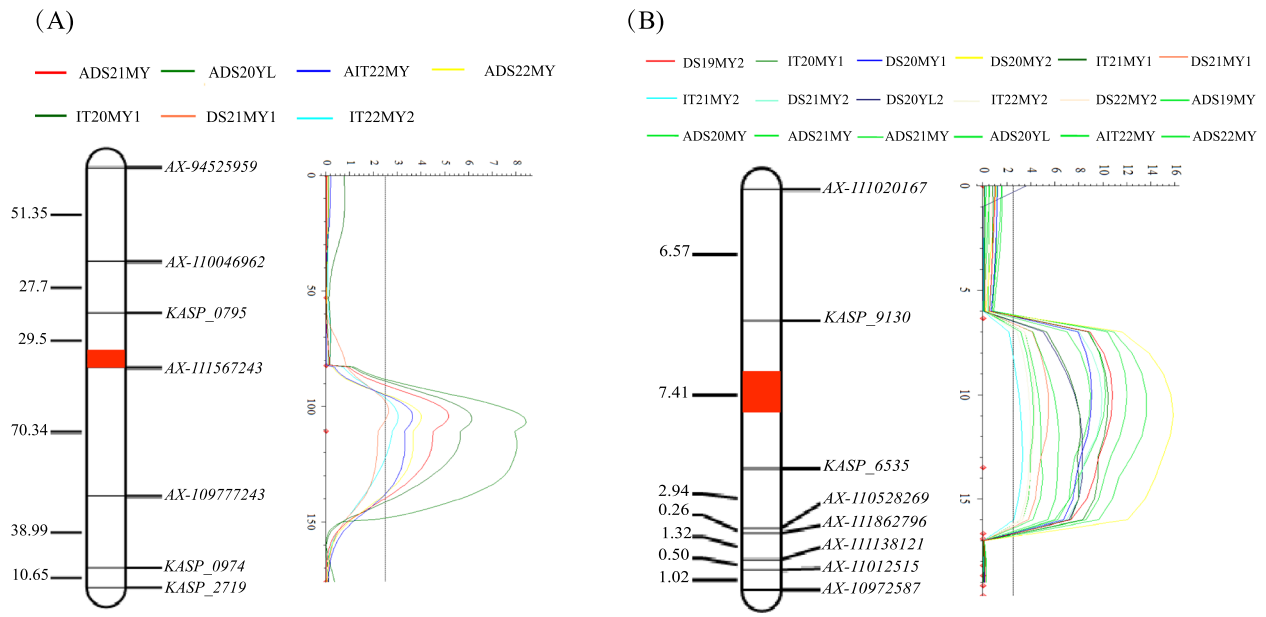

Fig. 3 Stripe rust resistance QTLs *QYr076.jaas-4D.1* (**A**) and *QYr076.jaas-4D.2* (**B**) on the genetic map of chromosomes 4D based on IT and DS data. The x-axis is in centimorgan distance (cM), and all genetic distance values shown are in the same scale; the y-axis indicates the LOD value. The red rectangle on the genetic map indicates the corresponding QTL region. AIT: The average of IT. ADS: average of DS

ufs-2A (Agenbag et al. 2012), *QYrva.vt-2AS_VA00W-38* (Christopher et al. 2013), *QYr.ucw-2AS_PI610750* (Lowe et al. 2011), *QYrtb.orz-2AS_cfd36* (Vazquez et al. 2015), *QYr.wpg-2A.1_gwm359* (Naruoka et al. 2015), *QYr.wpg-2A.2_IWA8274(*Naruoka et al. 2015*)*, *QYr.wpg-2A.3_IWA3047* (Naruoka et al. 2015), *QYr.wpg-2A.4_IWA7410* (Naruoka et al. 2015), *QYr.ucw-2A.3_IWA424* (Maccaferri et al. 2015), *QYr.wsu-2A.1_IWA2526* (Bulli et al. 2016), *QYr.wsu-2A.2_IWA5824* (Bulli et al. 2016), *YrTtd-2AS* (Liu et al. 2017), *Qyrww.wgp.2A-1* (Mu et al. 2020), *QYrzv.swust-2AS* (Zhou et al. 2021), *YrR61* (Hao et al. 2011), and *Qyr.gaas.2A* (Cheng et al. 2022). According to the physical location of molecular markers linked to the genes/QTLs, the general chromosome physical location of the genes/QTLs can be indirectly determined. Among these genes, *Yr17* was the only gene that showed both APR and ASR to stripe rust and was located in a region from 7.5 to 21.2 Mb (Beukert et al. 2020; Jia et al. 2011). *QYr.inra-2AS_CampRemy* was flanked by the SSR markers *Xwgm382a* and *Xgwm359*, which correspond to a physical location of approximately 28.20 Mb (Mallard et al. 2005). *QYr.inra_2AS.1_Recital* was flanked by *XDupw210* and *Xcfd36*, corresponding to the physical map region between 3.97 and 16.63 Mb (Dedryver et al. 2009). *QYr.sun-2A_Kukri* (Bariana et al. 2010), *QYr.ufs-2A* (Agenbag et al. 2012), *QYrst.orr-2AS_Stephens* (Dolores Vazquez et al. 2012), and *QYrva.vt-2AS_VA00W-38* (Christopher et al. 2013) were all in one small region and were flanked by the DArT marker *XwPt-0003*, which corresponds to the physical region of 29.94 Mb. *QYr.ucw-2AS_PI610750* was located between *XwPt-3896* (13.14 Mb) and *Xwmc177* (33.7 Mb) (Lowe et al. 2011). *QYrtb.orz-2AS_cfd36* was close to marker *Xcfd36* (16.63 Mb) (Vazquez et al. 2015). Naruoka et al. (2015) reported four QTLs, i.e., *QYr.wpg-2A.1_gwm359* (28.20 Mb), *QYr.wpg-2A.2_IWA8274* (16.55 Mb), *QYr.wpg-2A.3_IWA3047* (21.25 Mb) and *QYr.wpg-2A.4_IWA7410* (32.15 Mb) on the 2AS by a GWAS analysis. *QYr.ucw-2A.3_IWA424* was close to marker *XIWA424* (101.38 Mb) (Maccaferri et al. 2015). Bulli et al. (2016) reported *QYr.wsu-2A.1_IWA2526* and *QYr.wsu-2A.2_IWA5824*, corresponding to a physical location of approximately 36.63 and 77.53 Mb, respectively. *YrTtd-2AS* was close to marker *XIWB1046* (55.47 Mb) (Liu et al. 2017). *Qyrww.wgp.2A-1* was close to marker *IWB40903* (4.95 Mb) (Mu et al. 2020). *QYrzv.swust-2AS* was flanked by *IWB7877* and *IWB72720*, corresponding to 5.25–5.33 Mb (Zhou et al. 2021). QTL *QYr.uga-2AS_26R61*, corresponding to *YrR61* conferring APR to stripe rust, was flanked by the markers *Xbarc124* (3.78 Mb) and *Xgwm359* (28.20 Mb) (Hao et al. 2011). *QYrtm.pau-2A was* linked to *Xwmc407*, corresponding to the physical location of 28.2 Mb (Chhuneja et al. 2008). *QYr.GX-2AS* was flanked by the

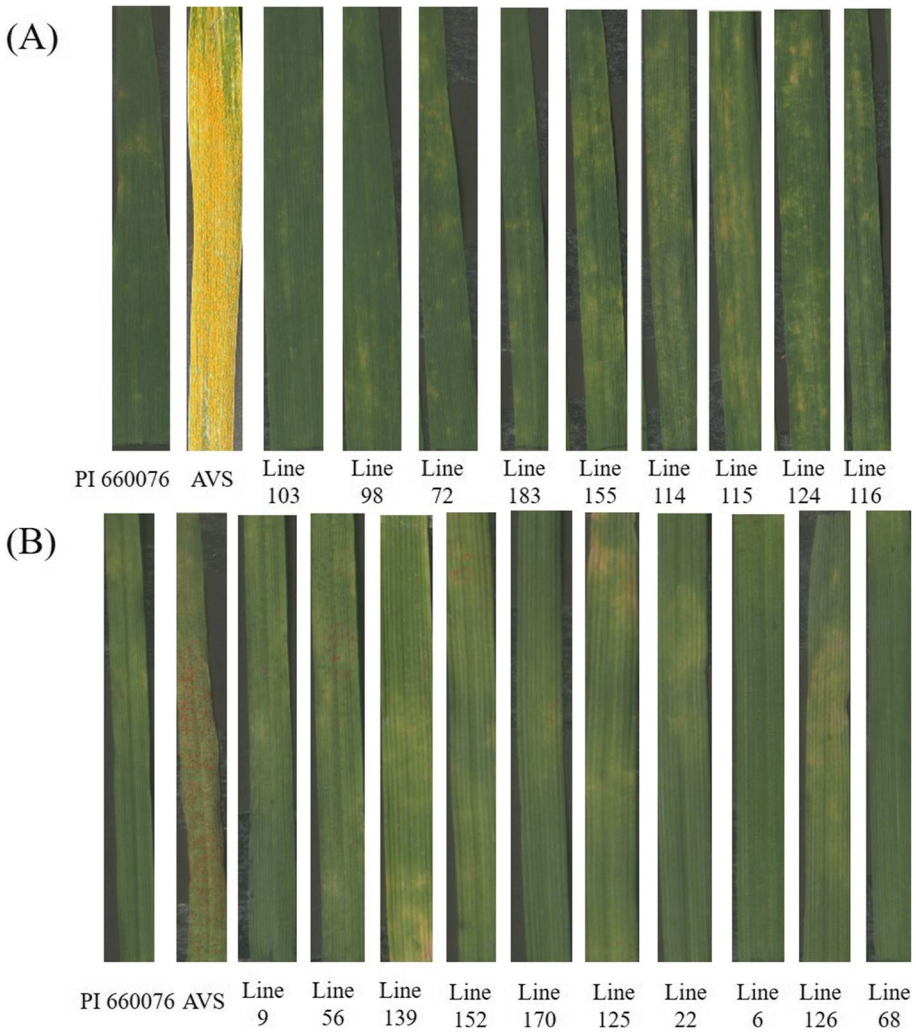

Fig. 4 Stripe rust reactions on the leaves of resistant parent PI660076, susceptible parent Avocet S (AvS), and representative stripe rust reactions of some of the recombinant inbred lines (RILs) in adult plants (**A**) and seedling plants (**B**) RIL lines containing single and homozygous *QYr076.jaas-2A*: line 6, line 9, line 68, line 125, line 139; RIL lines containing homozygous *QYr076.jaas-4D* (*QYr076.jaas-4D.1* and *QYr076.jaas-4D.2*): line 72, line 98, line 103, line 115, line 116, and line 183; RIL lines containing both *QYr076.jaas-2A* and *QYr076.jaas-4D* (*QYr076.jaas-4D.1* and *QYr076.jaas-4D.2*): line 22, line 56, line 124, line 126, line 152; RIL lines containing neither *QYr076.jaas-2A* or *QYr076.jaas-4D* (*QYr076.jaas-4D.1* and *QYr076.jaas-4D.2*): line 155, line 114, line 170

KASP markers *KP2A_37.09* and *KP2A_38.22*, which correspond to the physical map region between 37.09 and 38.22 Mb (Wang et al. 2021). *Qyr.gaas.2A* was mapped at the interval of *cfd36* ~ *AX-110576889* (16.63 ~ 31.85 Mb) (Cheng et al. 2022).

According to the physical locations of the linked markers of the QTL, the location and order of these QTLs on 2AS are as follows: *QYr.uga-2AS_26R61* (3.78 Mb)—*QYr.inra_2AS.1_Recital* (3.97 Mb)—*Qyrww.wgp.2A-1* (4.95 Mb)—*QYrzv.swust-2AS* (5.25 Mb)—*QYr.ucw-2AS_PI610750* (13.14 Mb)—*QYr.wpg-2A.2_IWA8274* (16.55 Mb)—*QYrtb.orz-2AS_cfd36* (16.63 Mb)—*QYr076.jaas-2A* (21.13 Mb)—*QYr.wpg-2A.3_IWA3047* (21.25 Mb)–*QYr.wpg-2A.1_gwm359* (28.2 Mb)—*QYr.inra-2AS_CampRemy* (28.2 Mb)—*QYrtm.pau-2A* (28.2 Mb)—*QYr.sun-2A_Kukri* (*QYr.ufs-2A*, *QYrst.orr-2AS_Stephens*, *QYrva.vt-2AS_VA00W-38*) (29.94 Mb)—*QYr.wpg-2A.4_IWA7410* (32.15 Mb)—*QYr.wsu-2A.1_IWA2526* (36.63 Mb)—*QYr.GX-2AS* (37.09 Mb)—*YrTtd-2AS* (55.47 Mb)—*QYr.wsu-2A.2_IWA5824* (77.53 Mb)—*QYr.ucw-2A.3_IWA424* (101.38 Mb). The relationship between *QYr076.jaas-2A* and nearby QTLs in the abovementioned region still needs to be confirmed with allelism tests.

Two QTLs (*QYr076.jaas-4D.1* and *QYr076.jaas-4D.2*) were mapped on chromosome 4D; however, there are few SNP markers on 4D; thus, the location range is still

Table 4 Summary of stripe rust resistance QTLs identified using ICIM based on the mean disease severity (DS) and infection type (IT) of the 119 RILs from the cross of AvS × PI660076 tested in Mianyang (MY) and Yangling (YL) in 2019–2022

Chromosome	Environments	Marker interval	IT			DS		
			[a]LOD	[b]PVE (%)	[c]Add	[a]LOD	[b]PVE (%)	[c]Add
2A	AIT19MY	*AX-110484643-KASP_4940*	5.34	11.26	-0.47	-	-	-
	ADS19MY	*AX-110484643-KASP_4940*	-	-	-	3.38	7.25	-5.18
	IT19MY1	*AX-110484643-KASP_4940*	3.32	7.13	-0.41	-	-	-
	DS19MY1	*AX-110484643-KASP_4940*	-	-	-	3.16	6.95	-5.79
	IT21MY1	*AX-110484643-KASP_4940*	8.24	16.58	-0.72	-	-	-
4D	ADS21MY	*KASP_0795-AX-111567243*	-	-	-	4.75	9.27	6.45
	ADS20YL	*KASP_0795-AX-111567243*	-	-	-	8.67	17.26	9.5
	AIT22MY	*KASP_0795-AX-111567243*	3.42	6.88	0.3	-	-	-
	ADS22MY	*KASP_0795-AX-111567243*	-	-	-	3.88	7.94	2.93
	IT20MY1	*KASP_0795-AX-111567243*	6.35	12.7	0.76	-	-	-
	IT22MY2	*KASP_0795-AX-111567243*	3.3	6.85	0.38	-	-	-
4D	ADS19MY	*KASP_9130-KASP_6535*	-	-	-	10.76	20.03	10.09
	ADS22MY	*KASP_9130-KASP_6535*	14.97	39.19	1.13	-	-	-
	ADS20MY	*KASP_9130-KASP_6535*	-	-	-	7.57	12.01	14.37
	AIT21MY	*KASP_9130-KASP_6535*	7.18	14.24	0.7	-	-	-
	ADS21MY	*KASP_9130-KASP_6535*	-	-	-	8.11	14.43	7.72
	ADS20YL	*KASP_9130-KASP_6535*	-	-	-	4.05	10.5	5.59
	AIT22MY	*KASP_9130-KASP_6535*	4.88	10.16	0.32	-	-	-
	IT20MY1	*KASP_9130-KASP_6535*	9.77	19	0.88	-	-	-
	DS20MY1	*KASP_9130-KASP_6535*	-	-	-	8	15.82	11.43
	IT21MY1	*KASP_9130-KASP_6535*	9.2	17.09	0.89			
	DS21MY1	*KASP_9130-KASP_6535*	-	-	-	4.77	8.77	6.14
	DS19MY2	*KASP_9130-KASP_6535*	-	-	-	11.2	20.55	10.61
	IT21MY2	*KASP_9130-KASP_6535*	3.84	8.24	0.52	-	-	-
	DS21MY2	*KASP_9130-KASP_6535*	-	-	-	9.14	16.46	9.17
	DS20YL2	*KASP_9130-KASP_6535*	-	-	-	7.2	18.71	8.43
	DS20MY2	*KASP_9130-KASP_6535*	4.18	7.97	0.24	-	-	-
	IT22MY2	*KASP_9130-KASP_6535*	4.26	8.97	0.39	-	-	-
	DS22MY2	*KASP_9130-KASP_6535*	-	-	-	4.38	9.28	3.76

[a] *LOD* logarithm of odds score

[b] *PVE* percentage of the phenotypic variance explained by individual QTLs

[c] *Add* additive effect of the resistance allele

large. To date, a total of seven stripe rust QTLs or genes on chromosome 4D have been reported, including *Yr28* (Singh et al. 2000) and *YrAS2388* (Huang et al. 2011) on 4DS, *QTL-4DL* from Israeli wheat Oligoculm (Suenaga et al. 2003), *Yr46* (Herrera-Foessel et al. 2011) (Sybil et al. 2010), *QYr.sun-4DL* (Chhetri et al. 2016) and *QYr.caas-4DL* (Lan et al. 2009; Ren et al. 2012b) on 4DL, and *Yr22* located on 4D, but the gene was not designated to a particular chromosomal location (Chen et al. 1995). Among these QTLs, *QYr.caas-4DL* and *Yr46* belong to adult plant resistance and are probably the same locus, but the relationship between the two loci has not yet been verified (Ren et al. 2012b), while the *QYr.sun-4DL* and *Yr46* genes have been confirmed to be the same (Herrera-Foessel et al. 2011). The *QTL-4DL* from Israeli wheat Oligoculm also confers APR, and this QTL was approximately 26 cM from *QYr.caas-4DL* (Suenaga et al. 2003). *Yr28* belongs to ASR, and Athiyannan et al. (2022) reported that *Yr28*, as well as the other two genes *YrAS2388* and *YrAet672*, were identified as haplotypes of the locus, all encoding identical protein sequences but are polymorphic in nontranslated regions of the gene. The gene *Yr22* also belongs to the ASR (Chen et al. 1995). Thus, based on the currently identified genes/QTLs, there are only 4 APR genes located on 4D, and the relationship between the QTLs on chromosome *4D* (*QYr076.jaas-4D.1* and *QYr076.jaas-4D.2*) and the three other QTLs still needs to be verified by subsequent relevant tests.

Table 5 Genetic (cM) and physical (Mb) positions of flanking markers of each QTL identified based on the mean infection type (IT) and disease severity (DS) of the 208 RILs from the AvS × PI660076 cross tested in Mianyang (MY) and Yangling (YL) in 2019–2022

QTL	Environments	Marker 1	Genetic Position (cM)	Physical Position (Mb)	Marker 2	Genetic Position (cM)	Physical Position (Mb)
2A	AIT19MY	*AX-89447915*	11	25.13	*KASP_4940*	11	21.13
	ADS19MY	*AX-110484643*	8	27.9	*AX-89447915*	8	25.13
	IT19MY1	*AX-110484643*	10	27.9	*AX-89447915*	10	25.13
	DS19MY1	*AX-110484643*	9	27.9	*AX-89447915*	9	25.13
	IT21MY1	*AX-89447915*	12	21.25	*KASP_4940*	12	21.13
4D	ADS21MY	*KASP_0795*	104	24.26	*AX-111567243*	104	46.99
	ADS20YL	*KASP_0795*	107	24.26	*AX-111567243*	107	46.99
	AIT22MY	*KASP_0795*	104	24.26	*AX-111567243*	104	46.99
	ADS22MY	*KASP_0795*	105	24.26	*AX-111567243*	105	46.99
	IT20MY1	*KASP_0795*	105	24.26	*AX-111567243*	105	46.99
	IT22MY2	*KASP_0795*	102	24.26	*AX-111567243*	102	46.99
4D	ADS19MY	*KASP_9130*	10	436.91	*KASP_6535*	10	379.78
	ADS22MY	*KASP_9130*	11	436.91	*KASP_6535*	11	379.78
	ADS20MY	*KASP_9130*	11	436.91	*KASP_6535*	11	379.78
	AIT21MY	*KASP_9130*	12	436.91	*KASP_6535*	12	379.78
	ADS21MY	*KASP_9130*	10	436.91	*KASP_6535*	10	379.78
	ADS20YL	*AX-111020167*	1	471.23	*KASP_9130*	1	436.91
	AIT22MY	*KASP_9130*	11	436.91	*KASP_6535*	11	379.78
	IT20MY1	*KASP_9130*	11	436.91	*KASP_6535*	11	379.78
	DS20MY1	*KASP_9130*	11	436.91	*KASP_6535*	11	379.78
	IT21MY1	*KASP_9130*	11	436.91	*KASP_6535*	11	379.78
	DS21MY1	*KASP_9130*	10	436.91	*KASP_6535*	10	379.78
	DS19MY2	*KASP_9130*	10	436.91	*KASP_6535*	10	379.78
	IT21MY2	*KASP_9130*	12	436.91	*KASP_6535*	12	379.78
	DS21MY2	*KASP_9130*	10	436.91	*KASP_6535*	10	379.78
	DS20YL2	*AX-111020167*	0	471.23	*KASP_9130*	0	436.91
	DS20MY2	*KASP_9130*	11	436.91	*KASP_6535*	11	379.78
	IT22MY2	*KASP_9130*	12	436.91	*KASP_6535*	12	379.78
	DS22MY2	*KASP_9130*	12	436.91	*KASP_6535*	12	379.78

Table 6 Information of the KASP markers developed in this study

	Primer sequence		
KASP markers	FAX	HEM	Common
KASP_4940	ACGGCCGTGTATACGTATTGGA	CGGCCGTGTATACGTATTGGC	CTTCATGGTCTTCAACCGGGTA
KASP_2719	CAACCCCCGCTGTTGCCGC	CAACCCCCGCTGTTGCCGT	GGTCGAAGATGCGGTGGGA
KASP_0974	CAAGGAAAAGCCGAAACCG	CAAGGAAAAGCCGAAACCC	CAACGTTTGCTCAAGAACTGGAT
KASP_9130	AAGGGGAAAAAAAGCCACTCCTT	AAGGGGAAAAAAAGCCACTCCTC	CCGGTGGTTGGCTATCTCTACGT
KASP_6535	TTGAATGGAAATACAGGCAGTGCA	TGAATGGAAATACAGGCAGTGCC	GTTTCCTTTTTTAATCGGTCAACCG
KASP_0795	CGGCCTTCATGTCTTCGCTA	CGGCCTTCATGTCTTCGCTC	CAAAGATACACATGCACACGAACA

Acknowledgements
The authors would like to thank Prof. Xianming Chen and Dr. Meinan Wang for providing the germplasm of PI660076 and invaluable advice and encouragement.

Authors' contributions
RR, XZ and PZ conceived and designed the research. JZ, YW and LW conducted the experiments, analyzed data. XL and SY participated in phenotypic and genotypic analyses of the RIL population. RR and XZ analyzed data and wrote the manuscript. All authors read and approved the final manuscript.

Funding
The authors acknowledge the National Natural Science Foundation of China (32272181, 32101707), the Key Research and Development Program of International Science and Technology Innovation Cooperation of Science and Technology Department of Sichuan Province, China (2022YFH0032), the Jiangsu Agricultural Science and Technology Innovation Fund (CX(21)3109).

Availability of data and materials
Plant materials and the datasets supporting the results of this article are included within the article.

Declarations

Ethics approval and consent to participate
Not applicable.

Consent for publication
Not applicable.

Competing interests
The authors declare that they have no competing interests.

Author details
[1]Institute of Food Crops, Provincial Key Laboratory of Agrobiology, Jiangsu Academy of Agricultural Sciences, Nanjing 210014, Jiangsu, China. [2]Scool of Life Sciences, Jiangsu University, Zhenjiang 212013, Jiangsu, China. [3]Wheat Research Institute, School of Life Sciences and Engineering, Southwest University of Science and Technology, Mianyang 621010, Sichuan, China. [4]School of Food and Biological Engineering, Jiangsu University, Zhenjiang 212013, Jiangsu, China. [5]Collaborative Innovation Center for Modern Crop Production Co-Sponsored By Province and Ministry, Nanjing 210014, Jiangsu, China.

Received: 2 January 2023 Accepted: 5 July 2023
Published online: 07 June 2024

References

Agenbag, G., Pretorius, Z., Boyd, L., Bender, C., & Prins, R. (2012). Identification of adult plant resistance to stripe rust in the wheat cultivar Cappelle-Desprez. *Theoretical and Applied Genetics, 125*, 109–120.

Athiyannan, N., Abrouk, M., Boshoff, W. H., Cauet, S., Rodde, N., Kudrna, D., Mohammed, N., Bettgenhaeuser, J., Botha, K. S., & Derman, S. S. (2022). Long-read genome sequencing of bread wheat facilitates disease resistance gene cloning. *Nature Genetics, 54*, 227–231.

Bariana, H., & McIntosh, R. (1993). Cytogenetic studies in wheat. XV. Location of rust resistance genes in VPM1 and their genetic linkage with other disease resistance genes in chromosome 2A. *Genome, 36*, 476–482.

Bariana, H., Bansal, U., Schmidt, A., Lehmensiek, A., Kaur, J., Miah, H., Howes, N., & McIntyre, C. (2010). Molecular mapping of adult plant stripe rust resistance in wheat and identification of pyramided QTL genotypes. *Euphytica, 176*, 251–260.

Beukert, U., Liu, G., Thorwarth, P., Boeven, P. H., Longin, C. F. H., Zhao, Y., Ganal, M., Serfling, A., Ordon, F., & Reif, J. C. (2020). The potential of hybrid breeding to enhance leaf rust and stripe rust resistance in wheat. *Theoretical and Applied Genetics, 133*, 2171–2181.

Bulli, P., Zhang, J., Chao, S., Chen, X., & Pumphrey, M. (2016). Genetic architecture of resistance to stripe rust in a global winter wheat germplasm collection. *G3: Genes. Genomes, Genetics, 6*, 2237–2253.

Chen, X. (2014). Integration of cultivar resistance and fungicide application for control of wheat stripe rust. *Canadian Journal of Plant Pathology, 36*, 311–326.

Chen, X. (2020). Pathogens which threaten food security: *Puccinia striiformis*, the wheat stripe rust pathogen. *Food Security, 12*, 239–251.

Chen, X., Jones, S., & Line, R. (1995). Chromosomal location of genes for stripe rust resistance in spring wheat cultivars Compair, Fielder, Lee, and Lemhi and interactions of aneuploid wheats with races of *Puccinia striiformis*. *Phytopathology, 85*, 375–381.

Cheng, B., Gao, X., Cao, N., Ding, Y., Chen, T., Zhou, Q., Gao, Y., Xin, Z., & Zhang, L. (2022). QTL mapping for adult plant resistance to wheat stripe rust in M96–5 × Guixie 3 wheat population. *Journal of Applied Genetics, 63*, 265–279.

Chhetri, M., Bariana, H., Kandiah, P., & Bansal, U. (2016). *Yr58*: A new stripe rust resistance gene and its interaction with *Yr46* for enhanced resistance. *Phytopathology, 106*, 1530–1534.

Chhuneja, P., Kaur, S., Garg, T., Ghai, M., Kaur, S., Prashar, M., Bains, N., Goel, R., Keller, B., & Dhaliwal, H. (2008). Mapping of adult plant stripe rust resistance genes in diploid A genome wheat species and their transfer to bread wheat. *Theoretical and Applied Genetics, 116*, 313–324.

Christopher, M. D., Liu, S., Hall, M. D., Marshall, D. S., Fountain, M. O., Johnson, J. W., Milus, E. A., Garland-Campbell, K. A., Chen, X., & Griffey, C. A. (2013). Identification and mapping of adult plant stripe rust resistance in soft red winter wheat VA00W-38. *Crop Science, 53*, 871–879.

Dedryver, F., Paillard, S., Mallard, S., Robert, O., Trottet, M., Negre, S., Verplancke, G., & Jahier, J. (2009). Characterization of genetic components involved in durable resistance to stripe rust in the bread wheat 'Renan.' *Phytopathology, 99*, 968–973.

Dolores, V. M., James, P. C., Riera-Lizarazu, O., Chen, X., Heesacker, A., Ammar, K., Crossa, J., & Mundt, C. C. (2012). Genetic analysis of adult plant, quantitative resistance to stripe rust in wheat cultivar 'Stephens' in multi-environment trials. *Theoretical and Applied Genetics, 124*, 1–11.

Dong, C., Zhang, L., Chen, Z., Xia, C., Gu, Y., Wang, J., Li, D., Xie, Z., Zhang, Q., Zhang, X., Gui, L., Liu, X., & Kong, X. (2020). Combining a new exome capture panel with an effective varBScore algorithm accelerates BSA-based gene cloning in wheat. *FRontiers in Plant Science, 11*, 1249.

Feng, J., Wang, M., See, D. R., Chao, S., Zheng, Y., & Chen, X. (2018). Characterization of novel gene *Yr79* and four additional quantitative trait loci for all-stage and high-temperature adult-plant resistance to stripe rust in spring wheat PI 182103. *Phytopathology, 108*, 737–747.

Hao, Y., Chen, Z., Wang, Y., Bland, D., Buck, J., Brown-Guedira, G., & Johnson, J. (2011). Characterization of a major QTL for adult plant resistance to stripe rust in US soft red winter wheat. *Theoretical and Applied Genetics, 123*, 1401–1411.

Herrera-Foessel, S. A., Lagudah, E. S., Huerta-Espino, J., Hayden, M. J., Bariana, H. S., Singh, D., & Singh, R. P. (2011). New slow-rusting leaf rust and stripe rust resistance genes *Lr67* and *Yr46* in wheat are pleiotropic or closely linked. *Theoretical and Applied Genetics, 122*, 239–249.

Huang, L., Zhang, L. Q., Liu, B. L., Yan, Z. H., Zhang, B., Zhang, H. G., Zheng, Y. L., & Liu, D. C. (2011). Molecular tagging of a stripe rust resistance gene in *Aegilops tauschii*. *Euphytica, 179*, 313–318.

Jia, J., Li, G., Liu, C., Lei, M., & Yang, Z. (2011). Characterization of wheat yellow rust resistance gene *Yr17* using EST-SSR and rice syntenic region. *Cereal Research Communications, 39*, 88–99.

Klymiuk, V., Chawla, H. S., Wiebe, K., Ens, J., Fatiukha, A., Govta, L., Fahima, T., & Pozniak, C. J. (2022). Discovery of stripe rust resistance with incomplete dominance in wild emmer wheat using bulked segregant analysis sequencing. *Communications Biology, 5*(1), 826. https://doi.org/10.1038/s42003-022-03773-3

Kosambi, D.D. (2016). The estimation of map distances from recombination values. In: DD Kosambi. Springer, pp 125–130.

Lan, C., Liang, S., Wang, Z., Yan, J., Zhang, Y., Xia, X., & He, Z. (2009). Quantitative trait loci mapping for adult-plant resistance to powdery mildew in Chinese wheat cultivar Bainong 64. *Phytopathology, 99*, 1121–1126.

Li, H., & Durbin, R. (2009). Fast and accurate short read alignment with Burrows-Wheeler transform. *Bioinformatics, 25*(14), 1754–1760.

Lin, F., & Chen, X. (2007). Genetics and molecular mapping of genes for race-specific all-stage resistance and non-race-specific high-temperature adult-plant resistance to stripe rust in spring wheat cultivar Alpowa. *Theoretical and Applied Genetics, 114*, 1277–1287.

Line, R. F. (2002). Stripe rust of wheat and barley in North America: a retrospective historical review. *Annual Review of Phytopathology, 40*, 75.

Liu, W., Maccaferri, M., Chen, X., Laghetti, G., Pignone, D., Pumphrey, M., & Tuberosa, R. (2017). Genome-wide association mapping reveals a rich

genetic architecture of stripe rust resistance loci in emmer wheat (*Triticum turgidum* ssp. *Dicoccum*). *Theoretical and Applied Genetics, 130*, 2249–2270.
Lowe, I., Cantu, D., & Dubcovsky, J. (2011). Durable resistance to the wheat rusts: integrating systems biology and traditional phenotype-based research methods to guide the deployment of resistance genes. *Euphytica, 179*, 69–79.
Maccaferri, M., Zhang, J., Bulli, P., Abate, Z., Chao, S., Cantu, D., Bossolini, E., Chen, X., Pumphrey, M., & Dubcovsky, J. (2015). A genome-wide association study of resistance to stripe rust (*Puccinia striiformis* f. sp. *Tritici*) in a worldwide collection of hexaploid spring wheat (*Triticum aestivum* L). *G3: Genes. Genomes, Genetics, 5*, 449–465.
Mallard, S., Gaudet, D., Aldeia, A., Abelard, C., Besnard, A. L., Sourdille, P., & Dedryver, F. (2005). Genetic analysis of durable resistance to yellow rust in bread wheat. *Theoretical and Applied Genetics, 110*, 1401–1409.
Meng, L., Li, H., Zhang, L., & Wang, J. (2015). QTL IciMapping: integrated software for genetic linkage map construction and quantitative trait locus mapping in biparental populations. *The Crop Journal, 3*, 269–283.
Mu, J., Liu, L., Liu, Y., Wang, M., See, D. R., Han, D., & Chen, X. (2020). Genome-wide association study and gene specific markers identified 51 genes or QTL for resistance to stripe rust in US winter wheat cultivars and breeding lines. *Frontiers in Plant Science, 11*, 998.
Naruoka, Y., Garland-Campbell, K., & Carter, A. (2015). Genome-wide association mapping for stripe rust (*Puccinia striiformis* f. sp. *Tritici*) in US Pacific Northwest winter wheat (*Triticum aestivum* L.). *Theoretical and Applied Genetics, 128*, 1083–1101.
Ren, R., Wang, M., Chen, X., & Zhang, Z. (2012a). Characterization and molecular mapping of *Yr52* for high-temperature adult-plant resistance to stripe rust in spring wheat germplasm PI 183527. *Theoretical and Applied Genetics, 125*, 847–857.
Ren, Y., Li, Z., He, Z., Wu, L., Bai, B., Lan, C., Wang, C., Zhou, G., Zhu, H., & Xia, X. (2012b). QTL mapping of adult-plant resistances to stripe rust and leaf rust in Chinese wheat cultivar Bainong 64. *Theoretical and Applied Genetics, 125*, 1253–1262.
Singh, R., Nelson, J., & Sorrells, M. (2000). Mapping *Yr28* and other genes for resistance to stripe rust in wheat. *Crop Science, 40*, 1148–1155.
Suenaga, K., Singh, R., Huerta-Espino, J., & William, H. (2003). Microsatellite markers for genes *Lr34/Yr18* and other quantitative trait loci for leaf rust and stripe rust resistance in bread wheat. *Phytopathology, 93*, 881–890.
Vazquez, M. D., Zemetra, R., Peterson, C. J., Chen, X. M., Heesacker, A., & Mundt, C. C. (2015). Multi-location wheat stripe rust QTL analysis: genetic background and epistatic interactions. *Theoretical and Applied Genetics, 128*, 1307–1318.
Voorrips, R. (2002). MapChart: software for the graphical presentation of linkage maps and QTLs. *Journal of Heredity, 93*, 77–78.
Wang, M., Chen, X., Xu, L., Cheng, P., & Bockelman, H. E. (2012). Registration of 70 common spring wheat germplasm lines resistant to stripe rust. *Journal of Plant Registrations, 6*, 104–110.
Wang, X., Han, R., Chen, Z., Li, J., Zhu, T., Guo, J., Xu, W., Zi, Y., Li, F., & Zhai, S. (2022). Identification and evaluation of wheat–*Aegilops bicornis* lines with resistance to powdery mildew and stripe rust. *Plant Disease, 106*, 864–871.
Wang, Y., Liang, F., Guan, F., Yao, F., Long, L., Zhao, X., Duan, L., Wu, Y., Li, H., & Li, W. (2021). Molecular mapping and analysis of an excellent quantitative trait loci conferring adult-plant resistance to stripe rust in chinese wheat landrace Gaoxianguangtoumai. *Frontiers in Plant Science*:2288.
Zhou, X., Du, J., & Yang, J. (2003). A 30 successive years' observation on the performance of several wheat cultivars in resistance to stripe rust (*Puccinia striiformis* West.) in the southern region of Gansu province of China. *Acta Phytopath Sinica, 33*, 550–554.
Zhou, X., Wang, M., Chen, X., Lu, Y., Kang, Z., & Jing, J. (2014). Identification of Yr59 conferring high-temperature adult-plant resistance to stripe rust in wheat germplasm PI 178759. *Theoretical and Applied Genetics, 127*, 935–945.
Zhou, X., Zhan, G., Huang, L., Han, D., & Kang, Z. (2015). Evaluation of resistance to stripe rust in eighty abroad spring wheat germplasms. *Sci Agric Sin, 8*, 1518–1526.
Zhou, X., Zhong, X., Roter, J., Li, X., Yao, Q., Yan, J., Yang, S., Guo, Q., Distelfeld, A., & Sela, H. (2021). Genome-wide mapping of loci for adult-plant resistance to stripe rust in durum wheat Svevo using the 90K SNP array. *Plant Disease, 105*, 879–888.
Zhou, X., Li, X., Han, D., Yang, S., Kang, Z., & Ren, R. (2022b). Genome-Wide QTL Mapping for Stripe Rust Resistance in Winter Wheat Pindong 34 Using a 90K SNP Array. *Frontiers in Plant Science, 2022*, 13.
Zhou, X., Fang, T., Li, K., Huang, K., Ma, C., Zhang, M., Li, X., Yang, S., Ren, R., & Zhang, P. (2022a). Yield losses associated with different levels of stripe rust resistance of commercial wheat cultivars in China. *Phytopathology*, PHYTO-07–21–0286-R.

Publisher's Note